

# Development of Quasi-Two-Dimensional Nb<sub>2</sub>O<sub>5</sub> for Functional Electrodes of Advanced Electrochemical Systems

S. Zhuiykov and E. Kats

**Abstract**—In recent times there has been a growing interest in the development of quasi-two-dimensional niobium pentoxide (Nb<sub>2</sub>O<sub>5</sub>) as a semiconductor for the potential electronic applications such as capacitors, filtration, dye-sensitized solar cells and gas sensing platforms. Therefore once the purpose is established, Nb<sub>2</sub>O<sub>5</sub> can be prepared in a number of nano- and sub-micron-structural morphologies that include rods, wires, belts and tubes. In this study films of Nb<sub>2</sub>O<sub>5</sub> were prepared on gold plated silicon substrate using spin-coating technique and subsequently by mechanical exfoliation. The reason this method was employed was to achieve layers of less than 15nm in thickness. The sintering temperature of the specimen was 800°C. The morphology and structural characteristics of the films were analyzed by Atomic Force Microscopy (AFM), Raman Spectroscopy, X-ray Photoelectron Spectroscopy (XPS).

**Keywords**—Mechanical exfoliation, niobium pentoxide, quasi-two-dimensional, semiconductor, sol-gel, spin-coating, two dimensional semiconductors.

## I. INTRODUCTION

DEVELOPMENT of quasi-two-dimensional (Q2D) nano-sheets of MoO<sub>3</sub> and WO<sub>3</sub> by mechanical exfoliation has already opened a new direction in science and technology: Q2D nano-crystals [1]. In regard to the semiconductor oxides with the layered structure, it was shown that the unprecedented properties of these Q2D crystals may be tailored by reduction of the band gap and/or increase in the mobility with intercalation by H<sup>+</sup> or Li<sup>+</sup>. The interest in nanostructured Nb<sub>2</sub>O<sub>5</sub> has been continuously increasing due to its multifaceted structural and functional properties. Nanostructured Nb<sub>2</sub>O<sub>5</sub> has a huge potential as an alternative to Ta<sub>2</sub>O<sub>5</sub> and TiO<sub>2</sub> in such electronic applications as photovoltaics and gas sensing platforms [2]. With wide band gap, Nb<sub>2</sub>O<sub>5</sub> is an *n*-type transitional metal semiconductor with an oxygen stoichiometry dependent bandgap ranging between 3.4 to 4.0 eV and high-*k* (between 33 to 40). Stoichiometric Nb<sub>2</sub>O<sub>5</sub> is an insulator (conductivity,  $\sigma = \sim 3 \times 10^{-6} \text{ Scm}^{-1}$ ) and converts into semiconducting state ( $\sigma = \sim 3 \times 10^{-3} \text{ Scm}^{-1}$ ) with a decrease in oxygen stoichiometry (Nb<sub>2</sub>O<sub>4.8</sub>). Niobium pentoxide exists in many polymorphic forms. H-Nb<sub>2</sub>O<sub>5</sub> (pseudo-hexagonal), O-Nb<sub>2</sub>O<sub>5</sub> (orthorhombic), T-Nb<sub>2</sub>O<sub>5</sub>

(tetragonal) and M-Nb<sub>2</sub>O<sub>5</sub> (monoclinic) are the most common crystallographic phases. Nb<sub>2</sub>O<sub>5</sub> is very resistive to the thermal shocks and thermo-cycling, possesses high melting point and wide working temperature range. The dielectric constant value, quite superior to the Ta<sub>2</sub>O<sub>5</sub> ( $\epsilon'_{\text{Nb}_2\text{O}_5} = 41$  vs  $\epsilon'_{\text{Ta}_2\text{O}_5} = 27$ ), and an almost half density (higher specific capacitance) are just some of the advantages for the passive electronic device components. Depending on applications, Nb<sub>2</sub>O<sub>5</sub> can be synthesized in various nano- and sub-micron morphologies that include wires, rods, belts, particles and tubes.

Although there are a number of procedures for sintering nanostructured Nb<sub>2</sub>O<sub>5</sub> with highly crystalline and stratified structures, the combination of sol-gel/exfoliation methods provides an important advantage for the development of Q2D nano-sheets since the mechanical exfoliation can be resulted in nano-crystals with the average thickness of ~10-25 nm. New approaches to the development of Q2D nano-sheets are particularly attractive as they are capable of producing Q2D nano-crystals with advanced properties in comparison with many other conventional semiconductor oxide nanostructures. So far separated implementation of sol-gel and exfoliation techniques for development of Q2D nano-sheets has been predominantly concentrated on either dichalcogenides or MoO<sub>3</sub> and WO<sub>3</sub> semiconductor metal oxides [3]-[7]. These recent research reports have confirmed that when the semiconductor oxides can be nanostructured and further exfoliated down to Q2D nano-crystals, their bandgap then could be fine-tuned down to the reasonable level acceptable by the most of electronic and functional device applications.

In this work it is reported for the first time a possibility of the development Q2D Nb<sub>2</sub>O<sub>5</sub> nano-sheets by combined sol-gel/exfoliation method. Moreover, a new approach is presented for mapping the electrical properties in Q2D nano-sheets with thickness below the 20 nanometers scale, with scanning probe microscopy measurements carried out in air and without damaging the sample by carefully controlling the tip-sample force. This is done by combining C-AFM and a new method that joins together the advantages of Intermittent Contact AFM (IC-AFM), *i.e.*, a spatial resolution below 20 nm and no sample damage, and C-AFM, *i.e.*, very high current sensitivity, and the possibility to record local *I-V* curves, allowing the analysis of charge transport properties. This new imaging mode, termed here time-resolved CSFS-AFM, also known as PeakForce TUNA™ is based on the simultaneous measurements of the topography and the current flowing between the tip and the sample from the real-time analysis of force-distance curves measured for a tip oscillating in the kHz

S. Zhuiykov is with the CSIRO, Materials Science and Engineering Division, 37 Graham Rd., Melbourne, VIC. 3190, Australia (phone: +61 3 9252 6236; e-mail: Serge.zhuiykov@csiro.au).

E. Kats is with the CSIRO, Materials Science and Engineering Division, 37 Graham Rd., Melbourne, VIC. 3190, Australia (e-mail: Eugene.kats@csiro.au).

regime, far below the resonance frequency of the cantilever. The images are reconstructed pixel by pixel in real-time by averaging force–distance data in a time scale similar to IC-AFM. This work also reveals for the first time the results derived by PeakForce TUNA™ on the developed Q2D Nb<sub>2</sub>O<sub>5</sub> nano-sheets and their interfaces with the detailed information between the morphology of nano-sheets, their grain boundaries and the obtained properties of Q2D Nb<sub>2</sub>O<sub>5</sub> nano-crystals providing direct comparison between the morphology and the electrical properties at the nanometre scale. Furthermore, it is investigated how the H<sup>+</sup> intercalation improves the electrical conductivity of the developed Q2D Nb<sub>2</sub>O<sub>5</sub> nano-sheets. Finally, CSFS-AFM is applied to those nano-crystals to unravel the details of the current distribution at the grain boundaries interface.

## II. PROCEDURE

The prepared Q2D Nb<sub>2</sub>O<sub>5</sub> nano-sheets were fabricated by three-step process: the initial deposition method was conducted via spin-coating, followed by annealing at 800°C and the last step in the sequence was that sintered Nb<sub>2</sub>O<sub>5</sub> was subjected to the mechanical exfoliation to achieve super thin layers. After the samples were sintered and removed from the oven, they were conditioned at room temperature for seven days. All the reagents used in fabrication Nb<sub>2</sub>O<sub>5</sub> nano-sheets were high-purity analytical grade and were applied as received. The main advantage of these Q2D nano-structures is that the electrochemical properties and morphological characteristics can be significantly improved by two factors: (1) controlling (reducing) the band gap by minimizing the thickness of nano-sheets and (2) increasing the mobility with intercalation by H<sup>+</sup> ions. The crystalline structures, surface morphologies and surface chemistry were examined by AFM, FTIR, Raman Spectroscopy and XPS.

Raman Spectroscopy was used to determine and identify the vibrational and rotational information regarding the chemical bonds and for this purpose μSense-L-532-B Laboratory Raman Analyser, US was employed. During the testing CCD detector was cooled down to -60°C. The spectra obtained were studied by RamanReader-M Software (Enwave Optronics Inc).

CSFS-AFM scanning probe technique combines the advantages of IC-AFM (in terms of spatial resolution) and C-AFM (in terms of current sensitivity). Similar to IC-AFM, the tip and the sample are intermittently brought into interaction while the sample is scanned. However, in CSFS-AFM, the feedback loop controls the force applied on the sample for each individual oscillation cycle. This direct force control protects the tip and the sample from scan-induced damage, but more importantly, it allows every tip–sample contact to be controlled and recorded to extract the current values while the tip–sample contact area is minimized. The two electrical modules are characterized by a very high sensitivity below 100 fA.

The oscillation frequency of the probe is set between 1 and 2 kHz, which is intermediate between IC-AFM (>50 kHz) and C-AFM (contact mode operation). This working frequency

allows for the recording of the current values with an acceptable signal-to-noise ratio. When the tip is approaching the surface, the attractive forces (usually *van der Waals*, electrostatic, or capillary forces) pull the cantilever down toward the surface. When the forces overcome the cantilever stiffness, the tip is attracted by the surface, resulting in the dip in the approach curve (snap-in). Then, the force increases until the Z position of the modulation reaches its lowest point. The force at this point is maintained constant by the system feedback during the interaction period. The tip then starts to withdraw and the force decreases until it reaches a minimum on the retract curve (pull-off), which coincides with the minimum contact force during the cycle. When the tip has come off the surface, no significant force acts on it. During scanning, a DC bias can be applied between the tip and the sample and the current passing through the sample when the contact is effective can be recorded.

The chemistry and crystal phase arrangement of the Nb<sub>2</sub>O<sub>5</sub> nano-sheet was studied by X-ray photoelectron spectroscopy (XPS) using an AXIS Ultra DLD spectrometer (Kratos Analytical Inc., Manchester, UK) with a monochromated Al K<sub>α</sub> source at a power of 180 W (15 kV × 12 mA), a hemispherical analyser operating in the fixed analyser transmission mode and the standard aperture (analysis area: 0.3 mm × 0.7 mm). The total pressure in the main vacuum chamber during analysis was less than 10<sup>-8</sup> mbar. Survey spectra were acquired at pass energy of 160 eV. The sample was analysed at an emission angle of 0° as measured from the surface normal. Assuming typical values for the electron attenuation length of relevant photoelectrons the XPS analysis depth (from which 95 % of the detected signal originates) ranges between 5 and 10 nm. Data processing was performed using CasaXPS processing software version 2.3.15 (Casa Software Ltd., Teignmouth, UK).

## III. RESULTS AND DISCUSSION

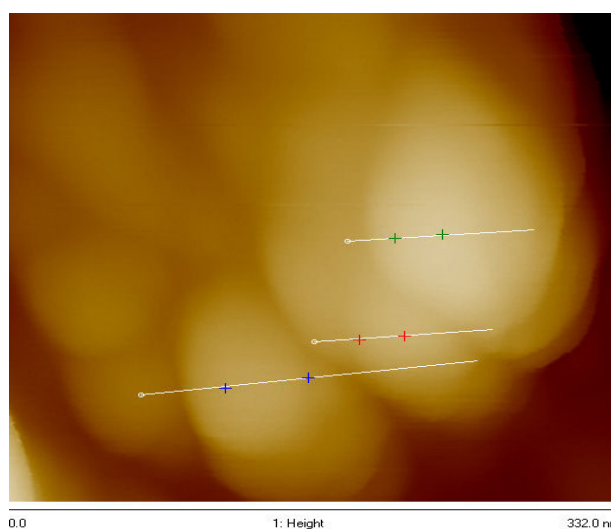


Fig. 1 AMF measurement of the developed structure of Q2D Nb<sub>2</sub>O<sub>5</sub> nano-sheets deposited on quartz. Insert – height measurements of the individual Nb<sub>2</sub>O<sub>5</sub> nano-sheets

Fig. 1 shows AFM measurements of the developed structure of quasi-2D  $\text{Nb}_2\text{O}_5$  nano-sheets deposited on quartz with height data of individual nano-sheets. As has been clearly shown in this figure, the exfoliated nano-sheets of  $\text{Nb}_2\text{O}_5$  still represent the layered structure consisting of 3 layers of  $\text{Nb}_2\text{O}_5$  nano-flakes with the average measured thickness from 15 to 25 nm.

At the edges between the different regions an increased Fowler-Nordheim tunneling current represented the dark areas on the image (Fig. 2 B). This indicates local structural thinning of the oxide during the fabrication, which serves as an insulating area between adjacent active regions. Enhanced current flow is noticeable along the grain boundaries of  $\text{Nb}_2\text{O}_5$  nano-sheet, whereas less current is observed on the individual nano-flakes. Significant contrast in colors for current/voltage measurements (Fig. 2 C) represents local variations in effective electrical thickness. It is evident that most often, areas with increased tunneling current seem to correspond with topographically elevated features. Analysis of adhesion image (Fig. 2 D) revealed that the developed Q2D nano-sheets had quite good adhesion to the quartz substrate (dark areas on nano-flakes, especially on those nano-flakes, which are directly contacted to the substrate).

Further investigation of the possibility of the progress of Q2D nano-sheets has shown that very small  $\text{Nb}_2\text{O}_5$  nano-sheets with dimensions of about  $40 \times 60$  nm and thickness as thin as  $\sim 5$  nm may also be developed. Fig. 3 depicts 3D AFM image of those  $\text{Nb}_2\text{O}_5$  nano-sheets on the quartz substrate with appropriate height measurements. In order to increase the mobility in the established Q2D  $\text{Nb}_2\text{O}_5$  nanostructures,  $\text{H}^+$  intercalation was completed by exposing these nano-sheets to the gas mixture (97%  $\text{N}_2$  + 3%  $\text{H}_2$ ) with controlled flow rate of  $200 \text{ cm}^3/\text{min}$ . The samples were mounted inside the chamber and were applied to the synthetic air for 30 min in order to remove any moisture and possible contaminants. Following this initial process, samples were subjected to the hydrogen-containing atmosphere for 5 min. After completion of the  $\text{H}^+$  intercalation, CV measurements were performed by using PF TUNA<sup>TM</sup> on several points of interest: from the edge to the middle of the Q2D  $\text{Nb}_2\text{O}_5$  sample. The summary results of these measurements are presented in Fig. 4.

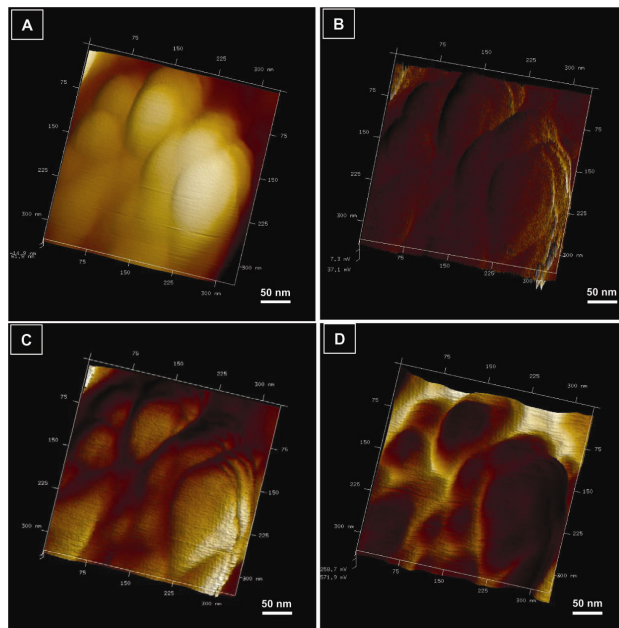


Fig. 2 Topography A, tunnelling B, current/voltage C and adhesion D images obtained simultaneously on Q2D  $\text{Nb}_2\text{O}_5$  nano-sheets deposited on quartz substrate

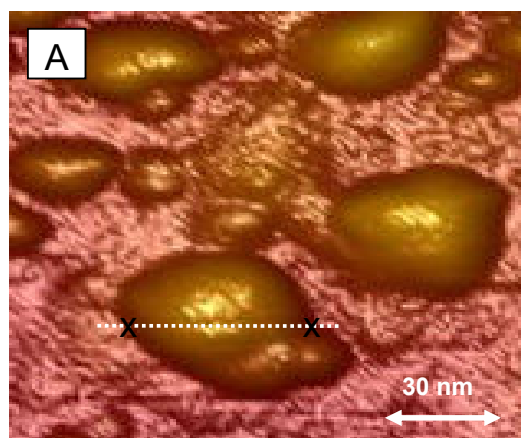


Fig. 3 3D AFM image of the developed Q2D  $\text{Nb}_2\text{O}_5$  nano-sheets deposited on quartz A with height measurements B

It is apparent that the  $H^+$  intercalation has increased conductivity of the Q2D  $Nb_2O_5$  sample particularly on the edges (positions 1 and 3). However, in the middle of the sample the conductivity has not been increased. In summary, we have synthesized Q2D nano-sheets of  $Nb_2O_5$  with average thickness of  $\sim 10$ - $25$  nm by using combined sol-gel/exfoliation method. Additional electrochemical testing of the  $Nb_2O_5$  samples intercalated by  $H^+$  provided clear evidence of increase in conductivity of nano-sheets and ability of their use as material for various sensing platforms with definite advantage to the carries mobility.

Raman spectroscopy was employed to determine the vibration and rotation information in relation to chemical bonds and symmetry of molecules in both the micro-structured  $Nb_2O_5$  film and Q2D  $Nb_2O_5$  nano-sheets, with particular interest to the finger-print region of the spectra, presented in Fig. 5 for both samples. In general terms the graphs not only display significant peaks in the perturbation area of the spectrum (Fig. 5 B), but also demonstrate a number of substantial stretches with various magnitude in the region of  $1400$ - $2000$   $cm^{-1}$ . Two stretches observed at  $482$   $cm^{-1}$  and  $1526$   $cm^{-1}$  correspond to Si and Au, respectively, which are part of the substrate itself. Broad peak detected at  $680$   $cm^{-1}$  confirms the presence  $Nb_2O_5$  for both spectra. However, the intensity of peak for Q2D  $Nb_2O_5$  nano-sheet was about three times higher than the intensity of the same peak for micro-structural  $Nb_2O_5$ . Distinctive peak observed at  $1462$   $cm^{-1}$ , confirmed the strong existence of C-N bonds. The spike at  $228$   $cm^{-1}$  indicated the presence of Nb-OH bond. There were no other peaks noted, suggesting that no impurities were present. Analysis of the FTIR spectra in Fig. 8 in addition to the Raman spectra in Fig. 3 confirms that Q2D  $Nb_2O_5$  nano-sheets are much for sensitive than micro-structured  $Nb_2O_5$  as component for the various plasmonic-based sensing platforms.

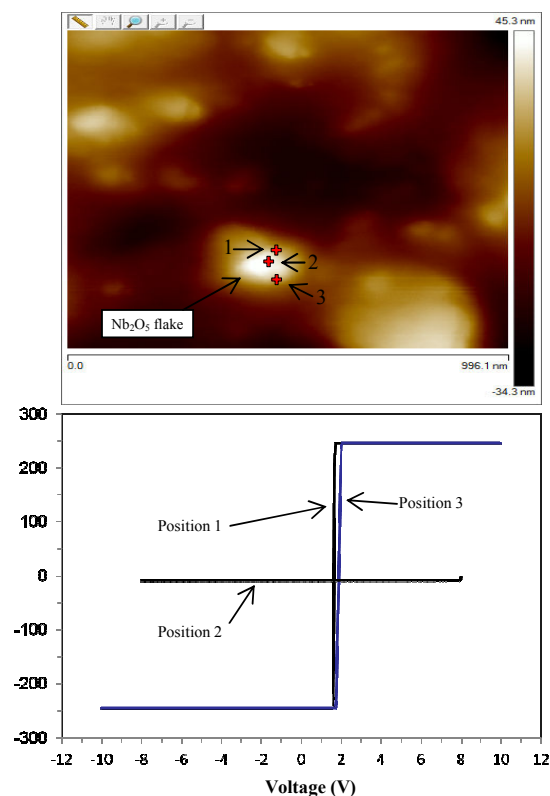


Fig. 4 PFTUNA<sup>TM</sup> AFM images for  $Nb_2O_5$  at three different positions on the flake with appropriate CV measurements for all three positions

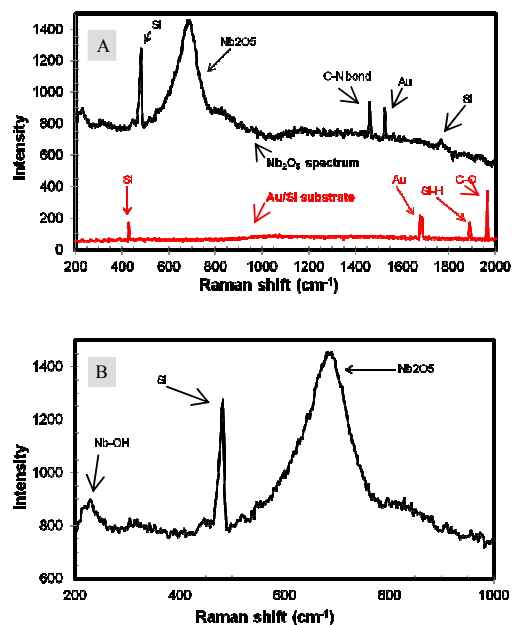


Fig. 5 Raman spectra for  $Nb_2O_5$  and Au/Si substrate reference A; perturbation region within  $200$ - $1000$   $cm^{-1}$  B

In this study XPS analysis was used for examination of the surface chemistry of Nb<sub>2</sub>O<sub>5</sub> nano-sheet by measuring its elemental composition and both chemical and electronic state of Nb and O within the sheet. XPS analysis of the Q2D Nb<sub>2</sub>O<sub>5</sub> nano-sheets, presented in Fig. 6, shows the characteristic binding energy shape of the core level spectra for Nb 3d shell electrons and O 1s shell electrons. Complimented EDS measurement of the Nb<sub>2</sub>O<sub>5</sub> nano-sheets (Fig. 7) clearly identifies niobium and oxygen as key components of the material. Due to the fact that the nano-sheets were not 100% dense, weak silica peaks were also observed. These signals are most probably because of the quartz substrate, which was used as a platform for all nano-sheets. As iridium was applied to coat the sample to improve the image quality, it is also present in the spectrum.

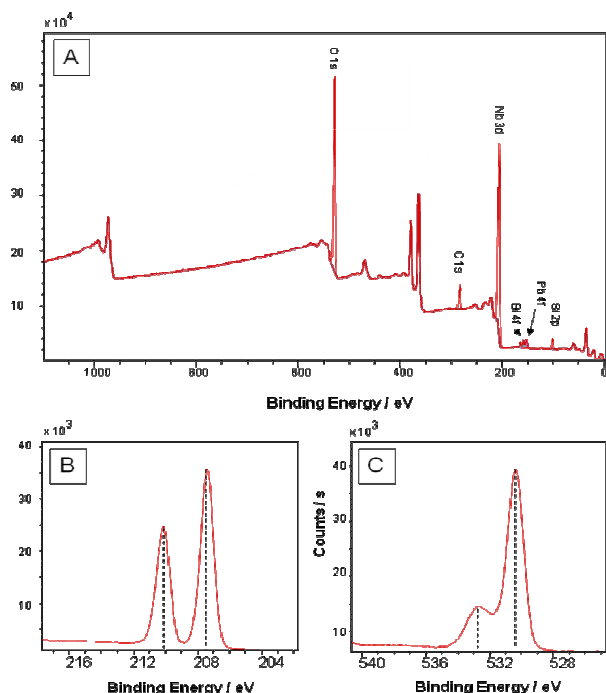


Fig. 6 XPS core level photoelectron peaks for Q2D Nb<sub>2</sub>O<sub>5</sub> nano-sheets: (A) spectrum, (B) Nb 3d, (C) O 1s

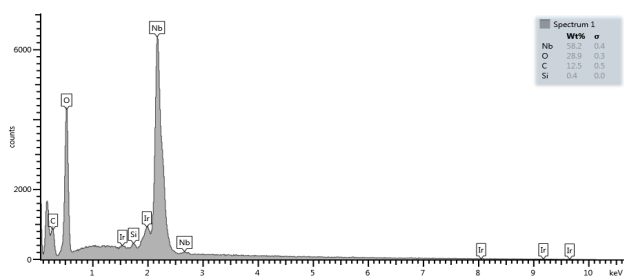


Fig. 7 EDS analysis of the developed Q2D Nb<sub>2</sub>O<sub>5</sub> nanostructure

#### IV. CONCLUSION

In summary, Q2D Nb<sub>2</sub>O<sub>5</sub> nano-sheets have been developed with the average thickness of ~15-25 nm using combination of the sol-gel/exfoliation techniques. Controllable increased conductivity of these Nb<sub>2</sub>O<sub>5</sub> nano-sheets can be achieved through the use of the appropriate H<sup>+</sup> intercalation process. It was confirmed that the Raman finger-prints from the Q2D Nb<sub>2</sub>O<sub>5</sub> nano-sheets were significantly amplified compared to the micro-structured Nb<sub>2</sub>O<sub>5</sub>, particularly in the low-frequency region. Additional electrochemical testing of the Nb<sub>2</sub>O<sub>5</sub> samples intercalated by H<sup>+</sup> provided clear evidence of the increase in conductivity of the developed nano-sheets and the ability of their use as a potential nano-material for various sensing platforms with definite advantage to the carrier mobility. Therefore, the presented Q2D Nb<sub>2</sub>O<sub>5</sub> nanostructures offer exciting opportunities in applications such as dye-sensitized solar cells, capacitors, photovoltaics, filtration and sensing platforms.

The nanoscale morphology and the electrical properties of the developed Nb<sub>2</sub>O<sub>5</sub> nano-sheets have also been studied in this research. The morphological analysis confirmed the tendency of Q2D Nb<sub>2</sub>O<sub>5</sub> nano-sheets to form multi-layers with common orientation. The combination of C-AFM and CSFS-AFM provided valuable information on the electrical properties of nano-material, showing that the current is governed by the spreading resistance at the tip-sample contact, resulting in high-resolution current contrast (below 10 nm) related to the local electrical properties of the investigated nano-materials. It was also possible to analyze simultaneously several characteristics not only the nano-material itself, but also its grain boundaries. The use of CSFS-AFM thus opens up the prospect of effective investigation of the electrical properties of nano-materials connected to their appropriate morphology at nanometer scale, i.e., where the phenomena actually occur, which is not possible to do by using the conventional AFM analysis.

#### ACKNOWLEDGMENT

The work was partially supported by the CSIRO Sensors and Sensor Networks Transformational Capability Platform (SSN TCP) and CSIRO Materials Science and Engineering Division.

#### REFERENCES

- [1] A.M. Taurino, A. Forleo, L. Francioso, P. Siciliano, M. Stalder and P. Nesper, "Synthesis, electrical characterization and gas sensing properties of molybdenum oxide nanorods", *Appl. Phys. Lett.*, vol. 88, pp.15211, 2006.
- [2] J.Z. Ou, R.A. Rani, M.H. Ham, M. R. Field, Y. Zhang, H. Zheng, P. Reece, S. Zhuiykov, S. Sriram, M. Bhaskaran, R.B. Kaner and K. Kalantar-zadeh, "Elevated temperature anodized Nb<sub>2</sub>O<sub>5</sub> - a photoanode material with exceptionally large photoconversion", *ASC Nano*, vol. 6, pp. 4045-4053, 2012.
- [3] S. Balendhran, J. Deng, J. Ou, S. Walia, J. Scott, J. Tang, K. Wang, M. Field, S. Russo, S. Zhuiykov, M. Strano, N. Medhekar, S. Sriram, M. Bhaskaran and K. Kalantar Zadeh, "Large carrier mobility in high-k two-dimensional metal oxides", *Advanced Materials*, vol. 25, pp.109-114, 2013.

- [4] S. Zhuiykov and E. Kats, "Atomically-thin two-dimensional materials for functional electrodes of electrochemical devices: A review," *Ionics*, vol. 19, pp.825-865, 2013.
- [5] Q. Zhang and G.Cao, "Nanostructured photoelectrodes for dye-sensitized solar cells," *Nano Today*, vol. 6, pp. 91-109, 2011.
- [6] M. D. Wei, Z. M Qi, M. Ichihara and H. S. Zhou, "Synthesis of single-crystal niobium pentoxide nanobelts," *Acta Mater.*, vol. 56, pp. 2488-2494, 2008.
- [7] J. Xia, N. Massaki, K. Jiang and S. Yanagida, "Fabrication and characterization of thin Nb<sub>2</sub>O<sub>5</sub> blocking layers for ionic liquid-based dye-sensitized solar cells," *J. Photochem Photobio A: Chem.*, vol. 188, pp. 120-127, 2007.

**Dr. Serge Zhuiykov** received his PhD in Materials Science and Engineering in 1991. He has combined experience as Research Scientist working at the different universities in Australia, Japan and Europe and industrial environments for more than 22 years. He is a Principal Research Scientist at Materials Science and Engineering Division of CSIRO. His research interests lie in the area of the development, design and evaluation of new functional materials for solid-state chemical sensors and other functional devices. He leads Sensors & Sensor Networks funded strategic co-investment CSIRO project. He is also Chairman of *FP-011-02* Technical Committee of Standards Australia International and a Head of the Australian delegation in International Standards Organization: *ISO TC21/SC8* Technical Committee since 2005. He has published 1 monograph, 5 chapters to books and more than 150 peer-reviewed scientific publications. He is a recipient of the 2007, 2011 Australian Academy of Science/Japan Society for Promotion of Science and 2010 Australian Government Endeavour Executive Awards for his work on chemical sensors based on advanced nanostructured semiconductors.